Mirkin, S. N., Lyamichev, V. I., Drushlyak, K. N., Dobrynin, V. N., Fillipov, S. A., & Frank-Kamenetskii, M. D. (1987) *Nature 330*, 495–497.
Morgan, A. R., & Wells, R. D. (1968) *J. Mol. Biol. 37*, 63–80.
Moser, H. E., & Dervan, P. B. (1987) *Science 238*, 645–650.
Nickol, J. M., & Felsenfeld, G. (1983) *Cell 35*, 467–477.
Patel, D. J., Shapiro, L., & Hare, D. (1987) *Q. Rev. Biophys. 20*, 35–112.
Plateau, P., & Gueron, M. (1982) *J. Am. Chem. Soc. 104*, 7310–7311.
Praseuth, D., Perrouault, L., Le Doan, T., Chassignol, M., Thuong, N., & Helene, C. (1988) *Proc. Natl. Acad. Sci. U.S.A. 85*, 1349–1353.
Reid, B. R. (1987) *Q. Rev. Biophys. 20*, 1–34.
Riley, M., Maling, B., & Chamberlin, M. J. (1966) *J. Mol. Biol. 20*, 359–389.
Schon, E., Evans, T., Welsh, J., & Efstratiadis, A. (1983) *Cell 35*, 837–848.
States, D. J., Haberkorn, R. A., & Ruben, D. J. (1982) *J. Magn. Reson. 48*, 286–292.
Van de Ven, F. J., & Hilbers, C. W. (1988) *Eur. J. Biochem. 178*, 1–38.
Voloshin, O. N., Mirkin, S. M., Lyamichev, V. I., Belotserkovskii, B. P., & Frank-Kamenetskii, M. D. (1988) *Nature 333*, 475–476.
Wells, R. D., Collier, D. A., Harvey, J. C., Shimizu, M., & Wohlrab, F. (1988) *FASEB J. 2*, 2939–2949.

Crystallographic Studies of the Mechanism of Xylose Isomerase†

Gregory K. Farber,‡ Arthur Glasfeld,‡ Gérard Tiraby,§ Dagmar Ringe,‡ and Gregory A. Petsko*,‡

Department of Chemistry, Massachusetts Institute of Technology, Cambridge, Massachusetts 02139, and Laboratoire de Microbiologie et Génétique Appliquées du CNRS, Université Paul Sabatier, F-31062 Toulouse Cedex, France

Received February 28, 1989; Revised Manuscript Received May 19, 1989

ABSTRACT: The mechanism of xylose isomerase (EC 5.3.1.5) has been studied with X-ray crystallography. Four refined crystal structures are reported at 3-Å resolution: native enzyme, enzyme + glucose, enzyme + glucose + Mg^{2+}, and enzyme + glucose + Mn^{2+}. One of these structures (E·G·Mg) was determined in a crystal mounted in a flow cell. The other structures were equilibrium experiments carried out by soaking crystals in substrate containing solution. These structures and other studies suggest that, contrary to expectation, xylose isomerase may not use the generally expected base-catalyzed enolization mechanism. A mechanism involving a hydride shift is consistent with the structures presented here and warrants further investigation. Additional evidence in support of a hydride shift comes from comparing xylose isomerase with triosephosphate isomerase which is known to catalyze an analogous reaction via an enediol intermediate. Evidence is presented that suggests that aldose–ketose isomerases can be divided into two groups. Phospho sugar isomerases generally do not require a metal ion for activity and show exchange of substrate protons with solvent. In contrast, simple sugar isomerases all require a metal ion and show very low solvent exchange. These observations are rationalized on the basis of the need for stereospecific sugar binding.

Using X-ray crystallography, we have embarked on a mechanistic study of xylose isomerase (EC 5.3.1.5) with the goal of uncovering the structural basis of its catalysis of the interconversion of xylose and xylulose. Extensive use of xylose isomerase (XyI) is made in industry for the production of high-fructose corn syrup by taking advantage of its fortuitous glucose isomerase activity (Layman, 1986). The enzyme may also prove useful in ethanol production from xylan-containing raw materials (Wilhelm & Hollenberg, 1984). Despite its industrial importance, relatively little is known about the mechanism of XyI.

Much of what has been assumed about the mechanism of xylose isomerase has been inferred by comparison with triosephosphate isomerase (TIM), which catalyzes a chemically analogous reaction, the isomerization of D-glyceraldehyde 3-phosphate to dihydroxyacetone phosphate, via an enediol intermediate (Albery & Knowles, 1976; Rose et al., 1969; Rose, 1981). These comparisons may be misleading. It has been shown that the true substrates for the reaction catalyzed by XyI are α-glucose (Schray & Rose, 1971) and α-fructose (Makkee et al., 1984). Therefore, before catalyzing isomerization, XyI must open the pyranose ring. Another difference between the two reactions is the phosphate group. TIM and other phospho sugar isomerases can use the phosphate group to orient and bind the sugar. The substrates for simple sugar isomerases have no equivalent chemical handle.

There are significant structural similarities between TIM and XyI. Both enzymes are eight-stranded α/β-barrels (Banner et al., 1975; Carrell et al., 1984; Farber et al., 1987), but XyI contains an additional C-terminal domain which is involved in intermolecular contacts. Despite the structural similarity and the analogous chemical transformations catalyzed by the two enzymes, some details of the kinetic behavior show marked difference. TIM requires no cofactor for catalysis and operates at the diffusion-controlled limit (Blacklow et al., 1988). In contrast, XyI requires divalent metal cations, usually Mg^{2+} or Mn^{2+}, for activity and has a k_{cat}/K_m 5 orders of magnitude lower than that of TIM (Suekane et al., 1978). In addition, TIM catalyzes the exchange of protons from

† This work was supported by NIH Grant GM26788 to G.A.P. and D.R.
‡ Massachusetts Institute of Technology.
§ Université Paul Sabatier.

0006-2960/89/0428-7289$01.50/0

substrate with solvent, but XyI appears to catalyze the hydrogen transfer from C1 to C2 of the sugar with no exchange of label (Rose et al., 1969; Rose, 1981). These dissimilarities could be indicative of mechanistic differences between TIM and XyI.

Although the catalytic mechanism of xylose isomerase has not been extensively studied, some aspects of the reaction pathway have been established. XyI is specific for the α-anomers of xylose, glucose, and fructose (Schray & Rose, 1971; Makkee et al., 1984). The hydrogen transfer between C1 and C2 proceeds suprafacially (Rose et al., 1969), and the isomerization of labeled substrate proceeds with exchange of the label occurring less than once in 10000 turnovers (Rose, 1981). There is an absolute requirement for a divalent metal ion (Suekane et al., 1978). The order of binding has been reported to be both ordered (Yamanaka, 1969) and random (Callens et al., 1986). Finally, the reaction is relatively slow. The turnover number for xylose is 10 s^{-1} and for glucose is 1 s^{-1}, compared with the rate of 8000 s^{-1} for TIM (Suekane et al., 1978; Krietsch et al., 1970).

Since xylose isomerase is a single-substrate/single product enzyme, it is possible to observe the Michaelis complex directly with X-ray crystallography. Substrate diffused into XyI crystals will bind to the active site and be converted to product, but product is just the substrate for the back-reaction. If one simply maintains a high concentration of substrate in the surrounding mother liquor, the time-averaged structure observed crystallographically will be whatever species predominates at equilibrium. The equilibrium constant for the XyI reaction on the enzyme is not known, so a priori one does not know whether to expect to see ES, EP, an intermediate between these complexes, or a mixture of these species.

The experiment can also be done at steady-state conditions by use of a flow cell (Petsko, 1985). In this case, a constant supply of one of the substrates is flowed over the crystal causing any product formed to be washed away. The time-averaged structure obtained in this experiment should be dominated by the species that precedes the transition state of highest free energy. That species may or may not be the same as that observed in the equilibrium experiment done by soaking the crystals in substrate.

In this paper, three crystal structures will be described: the enzyme–glucose–magnesium(II) complex (E·G·Mg), the enzyme–glucose–manganese(II) complex (E·G·Mn), and the enzyme–glucose complex with no metal (E·G). These structures have revealed an interesting disposition of residues in the active site with respect to bound sugar, as well as the possible role of the metal ion in catalysis. The crystallographic data, presented below, suggest the possibility of a 1,2-hydride shift mechanism in the isomerization of sugars by xylose isomerase.

Experimental Procedures

The crystal structure of native xylose isomerase from *Streptomyces olivochromogenes* has been reported previously (Farber et al., 1987). Since the completion of that work, the amino acid sequence (Tiraby et al., 1988) has been built into the electron-density map. The structure was then refined with the Konnert–Hendrickson least-squares refinement package (Hendrickson, 1985).

Two different methods were used to collect data on crystals of XyI with substrate. Data on the E·G·Mg structure were collected in a flow cell (Petsko, 1985). A solution containing 25 mM PIPES, 10 mM $MgCl_2$, 1 mM $CoCl_2$, 85% saturated $(NH_4)_2SO_4$, and 100 mM glucose at pH 7.5 was passed through the crystal during data collection. $CoCl_2$ was added to the mother liquor of both the native and the E·G·Mg crystals because it has been reported that Co^{2+} stabilizes xylose isomerase (Kasumi et al., 1982).

Table I: Summary of Refinement[a]

	native	E·G	E·G·Mg	E·G·Mn	target σ
bad distances[b]	901	989	716	678	
bond dist (Å)	0.015	0.016	0.014	0.013	0.020
angle dist (Å)	0.066	0.068	0.056	0.055	0.040
planar dist (Å)	0.064	0.066	0.060	0.059	0.050
planar restraint (Å)	0.015	0.016	0.007	0.006	0.020
chiral restraint (Å)	0.282	0.294	0.192	0.186	0.150
single torsion (Å)	0.315	0.315	0.302	0.300	0.450
planar torsion (deg)	3.7	4.0	12.6	12.3	5.0
R factor[c]	0.247	0.244	0.238	0.256	

[a] None of the structures had glucose or metal ions added to the model. [b] Bad distances are the number of bond lengths which are more than 0.04 Å from their ideal distance. There were 8231 distances in the molecule. [c] The R factor is $\sum(F_o - F_c)/\sum F_o$ in the 5.0–3.0-Å shell.

Binding of glucose in the crystal was monitored in the flow cell by collecting a set of *h0l* reflections to 3-Å resolution. To establish a reference data set, 391 reflections in this plane were collected with a solution of 25 mM PIPES, 10 mM $MgCl_2$, 1 mM $CoCl_2$, and 85% saturated $(NH_4)_2SO_4$ flowing through the crystal. This solution was then changed to the solution containing glucose. A small air bubble was introduced into the flow cell tubing between the two solutions to indicate when the glucose solution reached the crystal. As soon as the glucose solution reached the crystal, the unit cell changed slightly (from a = 98.92 Å, b = 93.77 Å, and c = 87.31 Å to a = 98.85 Å, b = 93.79 Å, and c = 87.06 Å). This small change necessitated a recentering of the crystal. The recentering took approximately 5 min. Immediately after recentering, the same set of *h0l* reflections was recollected. Several reflections had significant intensity changes compared to the first data set. The solution containing glucose was allowed to continue to flow through the crystal overnight. In the morning, the *h0l* reflections were collected for a third time. The intensities of the reflections in the third data set were the same as those in the second data set, and both sets were different from the first, pre-glucose, data set. These intensity changes as well as the unit cell changes suggested that glucose had bound to the enzyme. This experiment showed that in the crystal the binding of glucose occurs rapidly.

Structure determinations of XyI with glucose and with glucose plus Mn^{2+} were performed on crystals which had been soaked in substrate prior to mounting and data collection. The crystals used in these experiments were grown as previously described (Farber et al., 1987) with the following modifications. For the E·G structure, the crystals of the apoenzyme were grown from a solution to which no Mg^{2+} or Co^{2+} had been added. They were then soaked in a solution containing 25 mM PIPES, 50 mM glucose, and 62% saturated $(NH_4)_2SO_4$ at pH 7.5 for 24 h. A somewhat lower glucose concentration was used since the metal-free XyI crystals are not as mechanically stable as those crystals grown in the presence of metals. The XyI crystals for the E·G·Mn experiment were grown from a solution which contained Mn^{2+} as the sole metal ion. They were then soaked for 48 h in a solution containing 10 mM $MnCl_2$, 150 mM glucose, 65% saturated $(NH_4)_2SO_4$, and 25 mM PIPES at pH 7.5. The unit cell parameters for the three crystal forms are listed in Table II.

The data were collected on a Nicolet P3 diffractometer at ambient temperature with a sealed copper tube as the X-ray source. The methods of data collection and data reduction have been described elsewhere (Farber et al., 1987). Data

Table II: Summary of Data Collection[a]

	native	E·G	E·G·Mg	E·G·Mn
a (Å)	99.23	99.27	99.85	99.24
b (Å)	93.96	94.21	93.79	94.20
c (Å)	87.42	87.49	87.06	87.38
time in X-ray beam (h)	45, 50	77	105	116, 95
% decay[b]	30, 46	20	19	33, 17
isomorphous difference[c]		0.140	0.133	0.131
no. of reflections[d]	6682	6614	6150	6376

[a] The resolution range of all data sets was 44.0–3.0 Å. For the native and for the E·G·Mn data sets, both Friedel pairs were collected. This required two crystals for these data sets. The data from the two crystals for these sets were scaled together with a set of several hundred overlapping reflections. [b] The percent decay is the average decay of the five check reflections observed throughout data collection. Substrate binding appears to reduce the sensitivity of the crystals to X-rays. [c] Isomorphous difference is $\sum(F_{nat} - F_{deriv})/\sum F_{nat}$, the sums being taken over all common reflections. [d] This is the number of reflections in the $I222$ space group with intensity greater than 2σ. 6682 reflections is 78% of the number of possible reflections in this space group to 3-Å resolution.

collection is summarized in Table II.

All of these structures with substrate have been refined at 3-Å resolution. A summary of the final refinement statistics is given in Table I. Neither glucose nor metal ions were included in the refinement model. Therefore, the electron density shown in Figure 3 is not biased by any assumptions.

Results

A preliminary description of the structure of xylose isomerase has been given elsewhere (Farber et al., 1987). Since that publication, the amino acid sequence has been built into the electron-density map, and the structure has been refined. A more detailed description of xylose isomerase can now be given. A final description of the three-dimensional structure of xylose isomerase will be presented in a subsequent paper once the refinement at high resolution (2.2 Å) is complete.

Xylose isomerase has two domains. The first domain is an eight-stranded α/β-barrel composed of 307 amino acids (Figure 1). The second domain is a large loop of 70 amino acids. The second domain begins and ends with α-helices. The residues in the loop between these helices have little secondary structure. The 11 residues at the carboxy-terminal end of the enzyme are not visible in the electron-density map. Secondary structural features are listed in Table III.

In the crystal, two subunits of xylose isomerase form a tight dimer composed of the (x,y,z) and $(\bar{x},y,\bar{z})$ subunits. There are two distinct regions where these subunits interact. Along the barrel/barrel interface, helices 4, 5, and 6 in the (x,y,z) subunit make contact with, respectively, helices 6, 5, and 4 in the $(\bar{x},y,\bar{z})$ subunit. These three helices are hydrophobic. Eighty percent of the surface in this interface is made up of hydrophobic residues (Campbell, 1988).

The second interface region is composed of helices 3 and 4 from the (x,y,z) subunit and the second domain from the $(\bar{x},y,\bar{z})$ subunit. The amino-terminal end of helix 3 protrudes slightly through the second domain of the $(\bar{x},y,\bar{z})$ subunit (Figure 1).

Xylose isomerase has been reported to be both a dimer (Tucker et al., 1988) and a tetramer (Hogue-Angeletti, 1975). The crystal structure is consistent with these observations. In addition to the tight dimer described above, there is a second tight dimer that appears to form a tetramer in the crystal. The contacts between the tight dimers are not as extensive as the contacts between the subunits that form the tight dimer. It may be that while this tetramer readily forms in a high concentration environment (like a protein crystal), in solution the stable species is a dimer. This neighboring tight dimer is formed by the $(\bar{x},\bar{y}+1,z)$ and $(x,\bar{y}+1,\bar{z})$ subunits. These two dimers are oriented such that the carboxy-terminal ends of the α/β-barrels face each other. This tetramer is very similar to the tetramer of XyI from *Actinoplanes missouriensis* (Rey et al., 1988).

Table III: Secondary Structure of Xylose Isomerase

feature	residues[a]	feature	residues[a]
N-Terminal Domain (1–306)			
β1	10–17	β5	176–184
α1	36–42	α5	198–207
β2	48–54	β6	215–220
α2	64–71	α6	231–238
β3	82–88	β7	244–250
α3	101–119	α7	264–278
β4	123–128	β8	281–289
α4	144–157	α8	295–306
Small Secondary Features in the N-Terminal Domain			
αA	54–58	αB	136–139
C-Terminal Domain (307–377)			
αD	308–321	disordered	378–388
αE	363–367	residues	

[a] The numbering in this table starts with Ser as number 1.

Amino acid sequences are known for xylose isomerase from *Escherichia coli* (Schellenberg et al., 1983), *Bacillus subtilis* (Wilhelm & Hollenberg, 1985), *Ampullariella* strain 3876 (Saari et al., 1987), *Streptomyces violaceoniger* (Drocourt et al., 1988), and *S. olivochromogenes* (Tiraby et al., 1988). These sequences were aligned with the Needleman and Wunsch (1970) algorithm with a mutation data scoring matrix (Figure 2). Sixty two amino acids are identical in all five isomerases. Only five of these residues are in the second domain.

The location of the conserved residues is different between the first half of the α/β-barrel and the second half. In the first half of this domain, the four loops between β-strands and α-helices on the carboxy-terminal end of the barrel (residues 17–36, 54–64, 88–101, and 128–144) are strongly conserved. Two of these four loops (88–101 and 128–144) make contacts with the $(\bar{x},y,\bar{z})$ subunit in the tight dimer. The first loop (17–36) is involved in contacts with the neighboring tight dimer to form the tetramer. The last loop (54–64) allows access to the active site. In the second half of the barrel, the conserved residues are clustered on the β-sheets. These conserved residues make up the active site.

The glucose and metal ion binding site is buried deep in the interior of the enzyme toward the carboxy-terminal end of the barrel. The active site residues are located on the carboxy-terminal end of β-strands 5, 6, and 7 and in the loops which connect these β-strands with the α-helices on the outside of the barrel. Access to the active site is blocked on both ends of the α/β-barrel. Toward the amino-terminal end of the barrel, Met 83 and several other residues block the passage through the barrel. The carboxy-terminal end of the barrel is blocked by a ring of lysines and arginines and by the neighboring tight dimer. Since both ends of the barrel are restricted, the principal route to the active site is through a hole in the side of the α/β-barrel caused by a small helix (αA) perpendicular to the barrel axis formed by residues 54–58. This helix shortens β-strand 2 relative to the other seven strands that make up the barrel.

Figure 3a shows the active site residues from the refined E·G·Mg flow cell structure. There are three sets of residues in the active site. The set in closest proximity to bound glucose includes Ser 249, His 219, and Gln 221. These residues appear

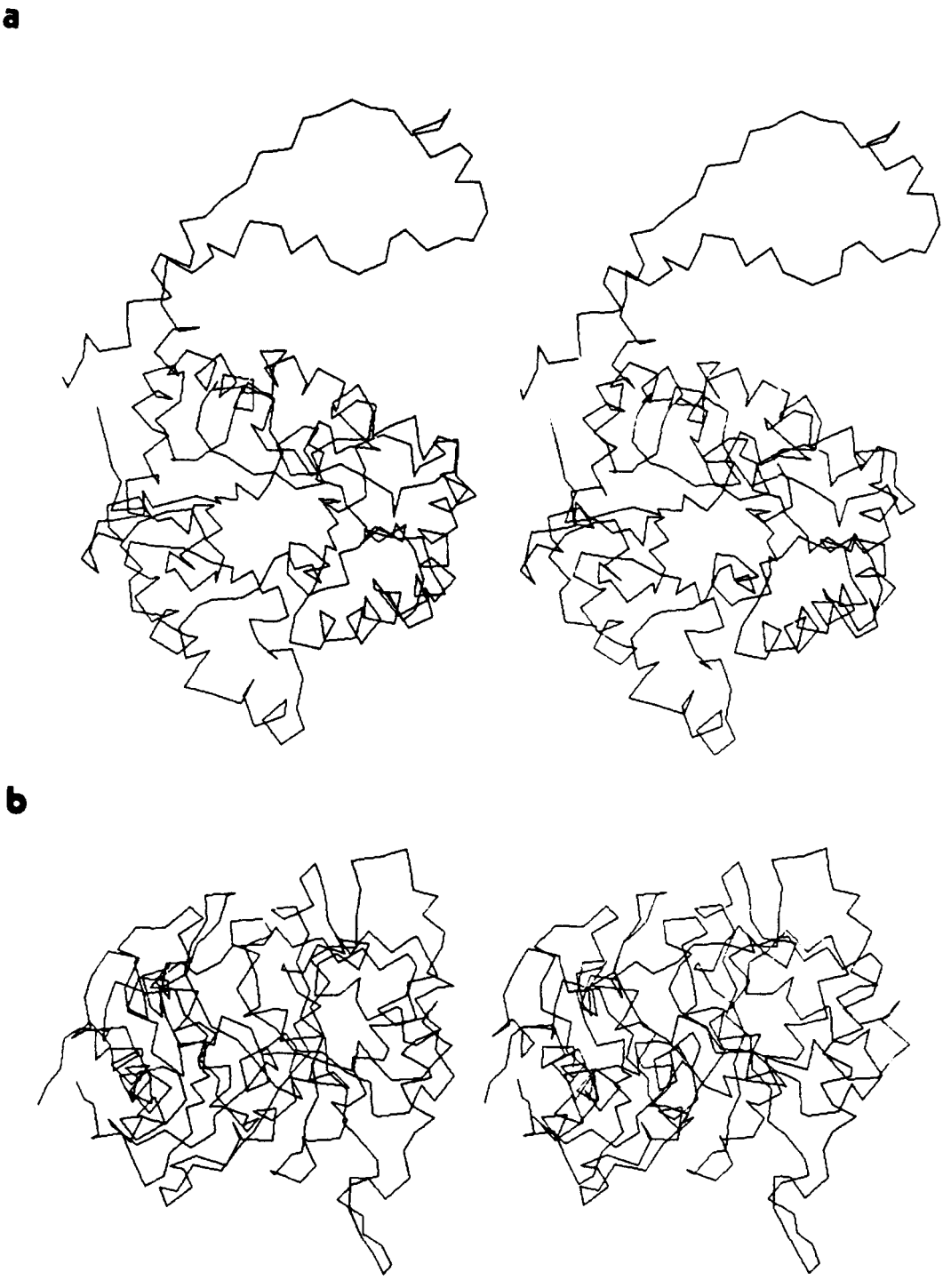

FIGURE 1: α-Carbon backbone of xylose isomerase. (a) This view of one subunit of xylose isomerase is from the carboxy-terminal end of the α/β-barrel parallel to the barrel axis. (b) This second view is perpendicular to the barrel axis. The small α-helix (54–58) that opens a hole into the active site is closest to the viewer.

to form a hydrogen-bonding network with His 219 at the center and the serine and glutamine flanking. His 219 seems likely to play a major role in catalysis. It is positioned to act either as a base in ring opening or in the transfer of a proton from C1 to C2 if catalysis by XyI goes by an enediol mechanism.

Slightly below His 219 (toward the N-terminal end of the barrel) and closer to the center of the β-barrel is a negatively charged set of residues which consists of Glu 180 and Asp 286. Structures b and c of Figure 3 show that these residues are involved in chelating the essential metal ion. Both Mg^{2+} and Co^{2+} were present in the native structure. However, no metal ion was seen in this structure. Therefore, it appears that the sugar is necessary for metal binding. Above this set (and above His 219) is the third set of residues, Lys 182 and Arg 258. The residues in the active site agree well with those determined by chemical labeling studies. Such studies have identified a single essential histidine residue and have suggested that thiols, lysine, and serine are not directly involved in the reaction (Gaikwad et al., 1988; Vangrysperre et al., 1988).

His 219, Glu 180, and Lys 182 are conserved in all five sequences. Gln 221 and Asp 286 are not strictly conserved. However, the changes at these positions are functionally conservative. The residues at position 221, Gln and Thr, can both form hydrogen bonds with His 219. Similarly, the residues at position 286, Asp and Asn, can both act as metal

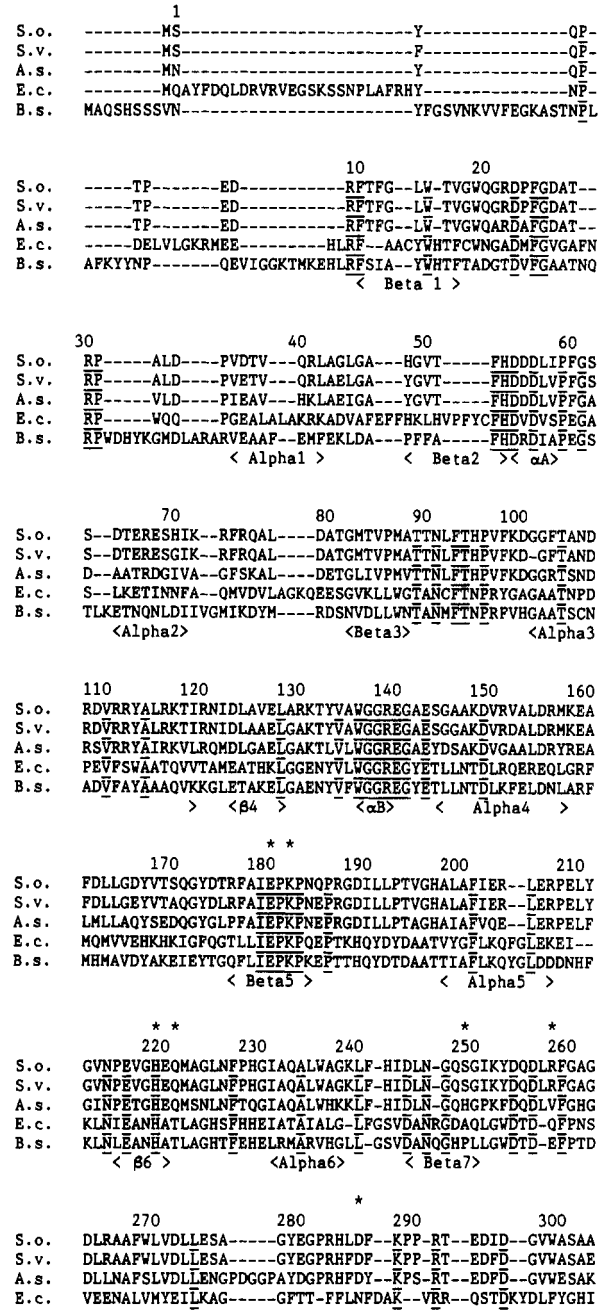

FIGURE 2: Alignment of xylose isomerase sequences. Abbreviations: S.o., *Streptomyces olivochromogenes*; S.v., *Streptomyces violaceoniger*; A.s., *Ampullariella* strain 3876; E.c., *Escherichia coli*; B.s., *Bacillus subtilis*. Standard single-letter code is used for the amino acids. The secondary structural features for *S. olivochromogenes* are listed below the amino acids. Those amino acids in the active site are marked with a star above the numbering. Underlined amino acids are conserved. The numbers refer to the *S. olivochromogenes* structure and start with Ser 1 since the N-terminal methionine is posttranslationally cleaved.

chelators. There are several gaps in the alignment in the region around 286. With only minor changes, it is possible to align the sequences to make Asp 286 strictly conserved. In contrast, the changes that occur at position 249 (Ser, His, Ala, Pro) and at position 258 (Arg, Val, Gln, Glu) are not conservative.

Figure 3b shows the electron density from the E·G·Mg flow cell structure. The density shows that the sugar is in a cyclic conformation in front of His 219. Because of the lack of detail at 3-Å resolution, it is impossible to decide which face of the sugar ring faces His 219. Moreover, the nature of the sugar species (be it α-glucose, fructose, or an open-chain intermediate in the isomerization process) cannot be identified from the electron-density map. The sugar electron density could be due to any or all of these species since the crystals are catalytically active (Farber, 1988).

In addition to the uncertainty in fitting the sugar density shown in Figure 3b, the possibility that the sugar and metal positions are reversed had to be considered. The crystal structure determination with Mn^{2+} in place of Mg^{2+} was performed in order to confirm our assignments. Manganese(II) has twice as many electrons as magnesium(II) so the electron density at the metal site should be significantly larger than the density shown in Figure 3b. The electron density for the E·G·Mn structure is shown in Figure 3c. Comparing structures b and c of Figure 3, one observes that the metal binds between Glu 180 and Asp 286, as expected. The metal ion also appears to be chelated by hydroxyl groups on the sugar.

The third, metal-free, structure (Figure 3d), xylose isomerase and glucose, contains electron density only at the sugar site. In contrast to the two other structures, the sugar density extends upward past Lys 182. The known structure of sorbitol (Ja Park et al., 1971), an open-chain glucose analogue with the carbonyl reduced to an alcohol, fits the electron density well, indicating that the sugar is bound in an extended form. This structure also provides an explanation for the inhibition of xylitol, which has been found to have a similar orientation in the active site of XyI (Farber, 1988). No electron density was observed in the metal site in the E·G structure.

As discussed earlier, the two different methods of data collection (flow cell and soaked crystal) can in principle show different aspects of the reaction as catalyzed by the enzyme. A soaked crystal will show electron density due to the equilibrium mixture of substrate, intermediate(s), and product. In contrast, the electron density in a flow cell experiment should be dominated by the species immediately preceding the rate-limiting step. Comparison of the E·G·Mg flow cell structure with the E·G·Mn structure shows some subtle differences in the sugar density. At 3-Å resolution, it is not possible to interpret these differences. However, it is probably safe to interpret the E·G·Mg electron density as showing that the rate-limiting step in the XyI reaction is preceded by a cyclic sugar form (with the ring either open or closed) rather than an extended sugar form. However, in the absence of a metal ion, the E·G structure shows that an open-chain form of the sugar has the lowest free energy when bound to the enzyme.

It is important to consider the possibility that parts of the sugar could be disordered in the crystal. In that case what appear to be cyclic sugar forms in the E·G·metal structures could be electron density due to only a small part of an extended sugar, for example, C1 through C3. The appearance of electron density in other enzyme–ligand compiex structures at this resolution suggests that the disordered extended sugar interpretation is less likely to be correct than that of a cyclic sugar coordinated to the metal through two adjacent oxygens.

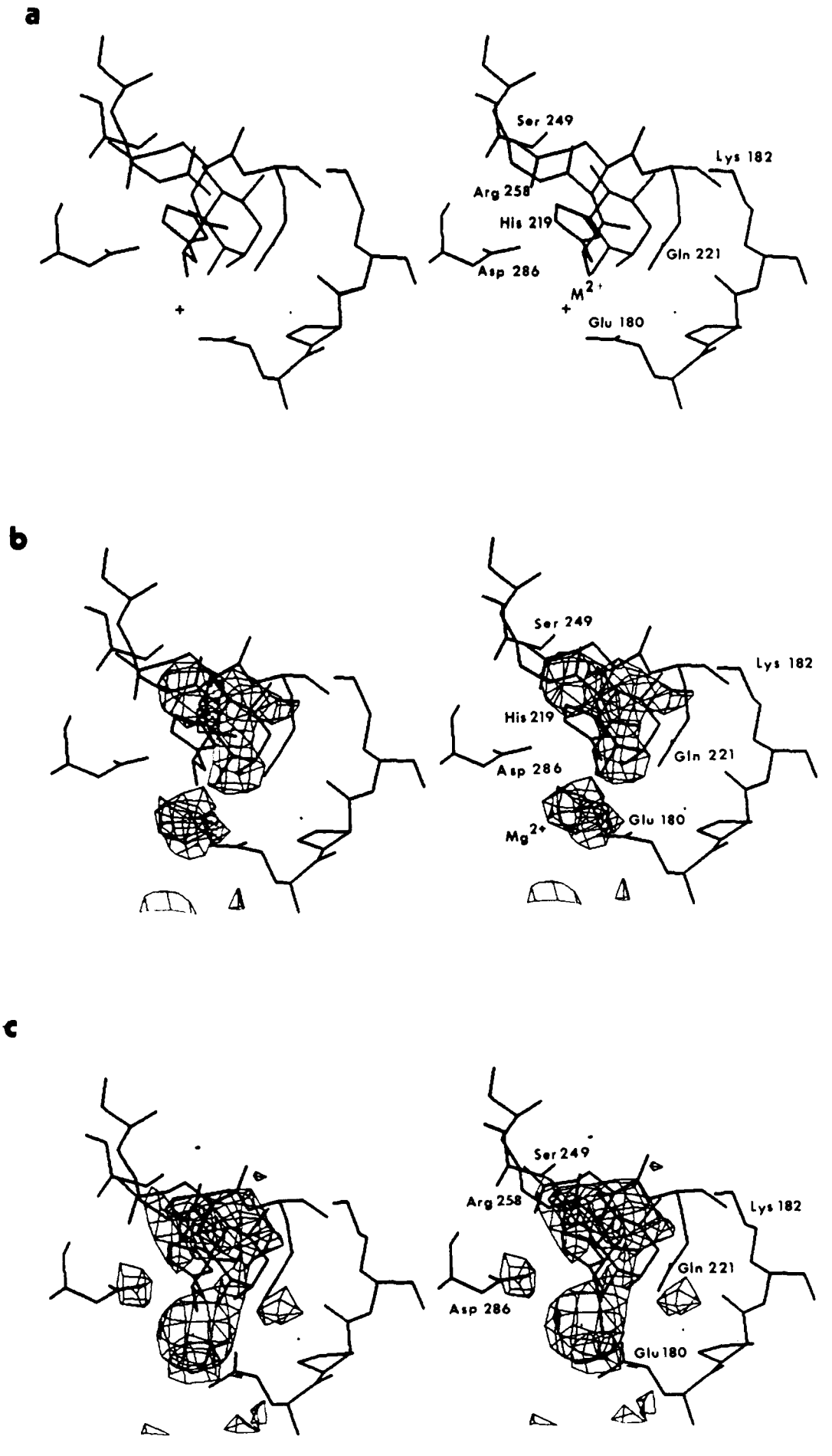
a
Ser 249
Lys 182
Arg 258
His 219
Gln 221
Asp 286
M^{2+}
Glu 180
b
Ser 249
Lys 182
His 219
Gln 221
Asp 286
Glu 180
Mg^{2+}
c
Ser 249
Arg 258
Lys 182
Gln 221
Asp 286
Glu 180

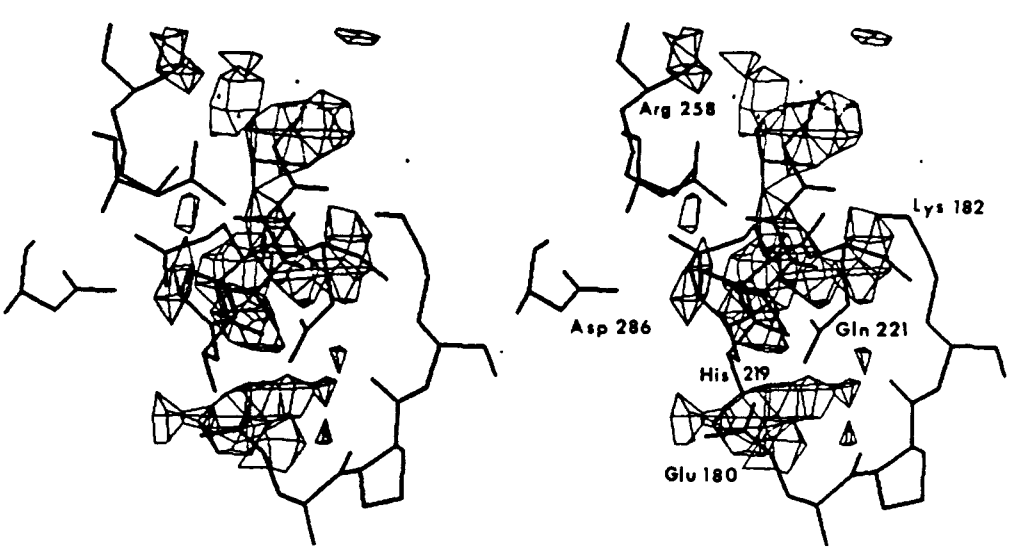

FIGURE 3: Active site of xylose isomerase. (a and b) These both show the refined E·G·Mg structure. Structure a has no electron density. The electron density in structure b comes from a $F_{Mg} - F_{nat}$ difference Fourier with native refined phases. The contour level is 1.7σ. The model for the sugar density is α-glucose. As discussed in the text, this model indicates only the sugar location and does not indicate the sugar orientation or identity. (c) This shows the refined E·G·Mn structure. The electron density shown here comes from a $F_{Mn} - F_{nat}$ difference Fourier with native refined phases. The contour level is 1.7σ, the same level as in structure b. Comparing this electron density to that in structure b shows that the metal ion chelates to Glu 180 and His 219. His 219 is behind the sugar and is not labeled. (d) This shows the refined E·G structure. The electron density shown here comes from a $F_{glucose} - F_{nat}$ difference Fourier with native refined phases. The contour level is 1.7σ. There is no density at the metal position, but the sorbitol model of open-chain glucose fits the density fairly well. Ser 249 is directly behind Arg 258 and is not labeled.

However, the mechanistic arguments presented in the next section depend only on the location of the sugar and not on its particular conformation.

Discussion

Despite the superficial similarity of the reaction catalyzed by XyI to the isomerization catalyzed by TIM, it may not be appropriate to assume that the two enzymes have the same mechanism. The principal kinetic objection to a proton-transfer mechanism with an enediol intermediate for XyI is the lack of exchange during a slow reaction. For comparison, TIM, which is known to have an enediol intermediate, has an exchange with solvent to intramolecular transfer ratio of 50 (Rose, 1981).

A possible rationale for this difference is that XyI may shield the active site from solvent more effectively than TIM. In fact, examples of proton-transfer reactions exist in which the enzyme shields the proton being transferred (Kozarich et al., 1981). If this were the case with XyI, the active site either should be inaccessible to solvent or should have a conformational change after substrate binding which prevents solvent from entering the active site. In xylose isomerase, the active site is indeed deeply buried in the enzyme. However, the flow cell experiment showed that crystalline xylose isomerase became saturated with glucose in less than 5 min. In an analogous experiment with TIM, substrate binding took over 1 h (Alber et al., 1981). These timing data are not directly comparable because TIM does undergo a conformational change upon substrate binding. However, the data do indicate that, in the crystal, the active site of XyI is accessible to substrate.

The lack of conformational change also suggests that xylose isomerase should have a more accessible active site than that of TIM. In TIM, once substrate binds, a loop folds down and covers the active site (Alber et al., 1981). No significant change occurs in the structure of XyI in any of the enzyme–substrate complexes described in this study. If TIM and XyI both have the same mechanism, these structural observations suggest that XyI should have an exchange to transfer ratio greater than that of TIM.

Further structural complications in a proton-transfer mechanism stem from the composition of the active site. There are four residues in the active site which are close enough to the sugar to be either the ring-opening base or the proton-transfer base: His 219, Glu 180, Asp 286, and Arg 258. Other residues near the active site could only be involved if there were substantial conformational changes of either substrate or enzyme during catalysis; no such motion is observed. Arg 258 can be excluded since a guanidinium group is a very unlikely base. Also, Arg 258 is the only one of these active site residues which is not conserved (Figure 2).

Since no exchange is observed during the isomerization, the proton-transfer base must be monoprotic. However, during the isomerization, Glu 180 and Asp 286 are chelated to the metal ion. This leaves only His 219 as the proton-transfer base. Histidine can certainly function as such a base, but if His 219 is the proton-transfer base, there is no obvious candidate for a ring-opening base. The E·G structure suggests that the enzyme is able to catalyze ring opening without a metal ion. In that structure, His 219 is positioned to act as the ring-opening base. It seems unlikely that the same residue is used as a base twice during the reaction on two different faces of the sugar ring.

Assigning the role of ring-opening base to Glu 180 or Asp 286 is a little better. If this were the case, one of these residues would have to open the sugar ring and then subsequently serve as a metal chelator. Substantial sugar movement would then be required to allow His 219 to act as the proton-transfer base once the sugar ring was open. This mechanism requires that sugar binding and ring opening precede metal binding.

The structures suggest a simpler proposition, that xylose isomerase might catalyze its reaction via a hydride shift mechanism. His 219 is thus solely the ring-opening base, and no proton-transfer base is required. The absence of exchange is consistent with hydride transfer. The essential divalent metal cation serves as a Lewis acid in this mechanism, stabilizing the formation of a carbocation ion at the carbonyl carbon prior to the concerted transfer of a hydrogen with two electrons. It

Table IV: Trends among Sugar Isomerases

isomerase	aldose, K_m (M)	ketose, K_m (M)	cofactor	turnover no. (s^{-1})	T/E[a]	ref
		Phospho Sugar Isomerases				
triosephosphate, EC 5.3.1.1	glyceraldehyde 3-P, 4.2×10^{-5}	dihydroxyacetone P, 6.8×10^{-4}	none	8000	50	Krietsch, 1975
D-ribose-5-P, EC 5.3.1.6	D-ribose 5-P, 2×10^{-3}	D-ribulose 5-P	none		high	Domagk & Alexander, 1975
D-mannose-6-P, EC 5.3.1.8	D-mannose 6-P, 1.35×10^{-3}	D-fructose 6-P	Zn^{2+}	616	1	Noltman, 1972
D-glucose-6-P, EC 5.3.1.9	D-glucose 6-P, 2.7×10^{-4}	D-fructose 6-P	none	1525	1	Hizukuri et al., 1975
D-arabinose-5-P, EC 5.3.1.13	D-arabinose 5-P, 2.0×10^{-3}	D-ribulose 5-P	none			Volk, 1966
D-galactose-6-P	D-galactose 6-P, 9.6×10^{-3}	D-tagatose 6-P, 1.9×10^{-3}	none	25		Anderson & Bissett, 1982
		Simple Sugar Isomerases				
D-arabinose, EC 5.3.1.3	D-arabinose, 0.160	D-ribulose	Mn^{2+}	25	low	Yamanaka & Izumori, 1975
L-arabinose, EC 5.3.1.4	L-arabinose, 0.060	L-ribulose	Mn^{2+}	200	low	Patrick & Lee, 1975
D-xylose, EC 5.3.1.5	D-xylose, 0.010	D-xylulose	Mg^{2+}	10	$>1 \times 10^{-4}$	Suekane et al., 1978
D-mannose, EC 5.3.1.7	D-mannose, 1.4×10^{-3}	D-fructose	Mn^{2+}			Noltman, 1972
L-rhamnose, EC 5.3.1.14	L-rhamnose, 7.0×10^{-4}	L-rhamnulose	Mn^{2+}			Domagk & Zech, 1966
D-lyxose, EC 5.3.1.15	D-lyxose	D-xylulose	Mn^{2+}	5		Anderson, 1966
D-ribose, EC 5.3.1.20	D-ribose, 4.0×10^{-3}	D-ribulose	Mn^{2+}	1		Elbein & Izumori, 1982

[a] T/E is the ratio of exchange with solvent to intramolecular hydrogen transfer. These values come from the review by Rose (1981).

also appears that the metal ion could play a conformational role by stabilizing an orientation at C1 and C2 that favors hydride shift. Metal ions are known to be used in this role in the Meerwein–Ponndorf–Verley Oppenauer reactions (Shiner & Whittaker, 1969; Warnhoff et al., 1980) and in intramolecular Cannizzaro reactions (Okuyama et al., 1982), both of which involve a hydride shift.

The necessity for a metal ion is consistent with the anomeric specificity of xylose isomerase. α-Glucose has two hydroxyl groups in the cis configuration at C1 and C2. The crystal structure of *myo*-inositol, which has the same configuration of oxygens as α-glucose at C1 through C4, with $MgCl_2$ shows that the Mg^{2+} chelates between O1 and O2 (Blank, 1973). In β-glucose, all alcohol groups are trans, so no such metal chelation is possible (Angyal, 1980).

It is of interest to note that among sugar isomerases two types of enzymes can be recognized (Table IV). Those that use phosphorylated sugars as the substrate virtually all show activity in the absence of metal ion. They also have exchange to intramolecular transfer ratios greater than 1 (Rose, 1981). In contrast, those enzymes using simple sugars as substrates show universal dependence on divalent metal ions for activity and extremely low E/T ratios (Rose, 1981). In addition, the binding of substrate to the simple sugar isomerases tends to be weak and the turnover tends to be slower than those with the phosphorylated sugar isomerases.

This evidence supports a link between exchange rate and metal ion dependence. The correlation cannot be explained by divergent evolution from a common ancestor, since no sequence homology has been found among pentose isomerases (Lin et al., 1985) or among phospho sugar isomerases (Miles & Guest, 1984). One explanation for this behavior is that the metal ion serves as a handle for the sugar and serendipitiously produces the mechanistic traits universal to the pentose isomerases.

Since static crystal structures cannot prove an enzymatic mechanism, it is prudent to make the suggestion of a hydride shift mechanism with reservations. Glyoxylase I, an enzyme catalyzing a similar intramolecular redox reaction, also requires divalent metal ions and proceeds without significant exchange of label to solvent. However, mechanistic studies performed by Kozarich and co-workers have uncovered the existence of a carbanionic intermediate typical of proton transfer in the reaction pathway (Kozarich et al., 1981), which indicates that the enediol intermediate in the enzyme is well shielded and probably short lived. The significant difference between this reaction and that catalyzed by xylose isomerase is that the nonenzymatic glyoxylase reaction clearly proceeds by an enediol mechanism in solution, even in the presence of Mg^{2+} (Hall et al., 1978). In contrast, there is evidence that nonenzymatic isomerization of glucose, mannose, and xylose in strongly acidic aqueous solutions (Harris & Feather, 1975; Ralapati & Feather, 1978) involves a hydride shift mechanism as does the base-catalyzed isomerization of ribose (Gleason & Barker, 1971).

The evidence presented in this paper suggests that, contrary to expectation, not all sugar isomerases may proceed by the enediol mechanism that has been shown for TIM. In the case of xylose isomerase, a series of crystal structures combined with other evidence has suggested that a hydride shift mechanism should be considered. The mechanistic arguments presented in this paper depend only on the location of the active site and on the number and types of residues close to the sugar. All of these details are unambiguous at 3-Å resolution. Structures at higher resolution are not likely to aid in the understanding of the mechanism without other information. Until the free energy profile of the reaction catalyzed by xylose isomerase is elucidated, it will not be possible to decide how many and what type of sugars should be built into the electron density of these catalytically active crystals. Hopefully, this paper will encourage such studies.

ACKNOWLEDGMENTS

We thank Robert Campbell and David Volkin for helpful

discussions. The refined coordinates for the native structure at 3-Å resolution have been deposited in the Protein Data Bank.

References

Alber, T., Banner, D. W., Bloomer, A. C., Petsko, G. A., Phillips, D., Rivers, P. S., & Wilson, I. A. (1981) *Philos. Trans. R. Soc. London B293*, 159.

Albery, J., & Knowles, J. R. (1976) *Biochemistry 15*, 5627.

Anderson, R. L. (1966) *Methods Enzymol. 9*, 593.

Anderson, R. L., & Bissett, D. L. (1982) *Methods Enzymol. 89*, 562.

Angyal, S. J. (1980) *Chem. Soc. Rev. 9*, 415.

Banner, D. W., Bloomer, A. C., Petsko, G. A., Phillips, D. C., Pogson, C. I., & Wilson, I. A. (1975) *Nature (London) 255*, 609.

Blacklow, S. C., Raines, R. T., Lim, W. A., Zamore, P. D., & Knowles, J. R. (1988) *Biochemistry 27*, 1158.

Blank, G. (1973) *Acta Crystallogr. B29*, 1677.

Callens, M., Kersters-Hilderson, H., Opstol, O. V., & DeBruyne, C. K. (1986) *Enzyme Microb. Technol. 8*, 696.

Campbell, R. L. (1988) Analysis of Structural Features of Protein Surfaces, Ph.D. Thesis, Massachusetts Institute of Technology, p 111.

Carrell, H. L., Rubin, B. H., Hurley, T. J., & Glusker, J. P. (1984) *J. Biol. Chem. 259*, 3230.

Domagk, G. F., & Zech, R. (1966) *Methods Enzymol. 9*, 579.

Domagk, G. F., & Alexander, W. R. (1975) *Methods Enzymol. 41*, 424.

Drocourt, D., Bejar, S., Calmels, T., Reynes, J. P., & Tiraby, G. (1988) *Nucleic Acids Res. 16*, 9337.

Elbein, A. D., & Izumori, K. (1982) *Methods Enzymol. 89*, 547.

Farber, G. K. (1988) The Structure and Mechanism of Xylose Isomerase, Ph.D. Thesis, Massachusetts Institute of Technology.

Farber, G. K., Petsko, G. A., & Ringe, D. (1987) *Protein Eng. 1*, 459.

Gaikwad, S. M., More, M. W., Vartak, H. G., & Deshpande, V. V. (1988) *Biochem. Biophys. Res. Commun. 155*, 270.

Gleason, W. B., & Barker, R. (1971) *Can. J. Chem. 49*, 1433.

Hall, S. S., Doweyko, A. M., & Jordan, F. (1978) *J. Am. Chem. Soc. 100*, 5934.

Harris, D. W., & Feather, M. S. (1975) *J. Am. Chem. Soc. 97*, 178.

Hendrickson, W. A. (1985) *Methods Enzymol. 115*, 252.

Hizukuri, S., Takeda, Y., & Nikuni, Z. (1975) *Methods Enzymol. 41*, 388.

Hogue-Angeletti, R. A. (1975) *J. Biol. Chem. 250*, 7814.

Ja Park, Y., Jeffery, G. A., & Hamilton, W. C. (1971) *Acta Crystallogr. B27*, 2393.

Kasumi, T., Hayashi, K., & Tsumura, N. (1982) *Agric. Biol. Chem. 46*, 21.

Kozarich, J. W., Chari, R. V. J., Wu, J. C., & Lawrence, T. L. (1981) *J. Am. Chem. Soc. 103*, 4593.

Krietsch, W. K. G. (1975) *Methods Enzymol. 92*, 434.

Krietsch, W. K. G., Pentchev, P. G., Klingenburg, H., Hofstatter, T., & Bucher, T. (1970) *Eur. J. Biochem. 14*, 289.

Layman, P. L. (1986) *Chem. Eng. News 64(37)*, 1.

Lin, H.-C., Lei, S.-P., & Wilcox, G. (1985) *Gene 34*, 123.

Makkee, M., Kleboom, A. P. G., & van Bekkum, H. (1984) *Recl. Trav. Chim. Pays-Bas 103*, 361.

Miles, J. S., & Guest, J. R. (1984) *Gene 32*, 41.

Needleman, S. B., & Wunsch, C. D. (1970) *J. Mol. Biol. 48*, 443.

Noltman, E. A. (1972) *Enzymes (3rd Ed.) 6*, 302.

Okuyama, T., Kimura, K., & Fueno, T. (1982) *Bull. Chem. Soc. Jpn. 55*, 2285.

Patrick, J., & Lee, N. (1975) *Methods Enzymol. 92*, 453.

Petsko, G. A. (1985) *Methods Enzymol. 114*, 141.

Ralapati, S., & Feather, M. S. (1978) *J. Carbohydr., Nucleosides, Nucleotides 5*, 297.

Rey, F., Jenkins, J., Janin, J., Lasters, I., Alard, P., Claessens, M., Matthyssens, G., & Wodak, S. (1988) *Proteins 4*, 165.

Rose, I. A. (1981) *Philos. Trans. R. Soc. London B293*, 131.

Rose, I. A., O'Connell, E. L., & Mortlock, R. P. (1969) *Biochim. Biophys. Acta 178*, 376.

Saari, G. C., Kumar, A. A., Kawasaki, G. H., Insley, M. Y., & O'Hara, P. J. (1987) *J. Bacteriol. 169*, 612.

Schellenberg, G. D., Sarthy, A., Larson, A. E., Backer, M. P., Crabb, J. W., Lindstrom, M., Hall, B. D., & Furlong, C. E. (1983) *J. Biol. Chem. 255*, 6826.

Schray, K. J., & Rose, I. A. (1971) *Biochemistry 10*, 1058.

Shiner, V. J., & Whittaker, D. (1969) *J. Am. Chem. Soc. 91*, 394.

Suekane, M., Tamura, M., & Tomimura, C. (1978) *Agric. Biol. Chem. 42*, 909.

Tiraby, G., Bejar, S., Drocourt, D., Reynes, J. P., Sicard, P. J., Farber, G. K., Glasfeld, A., Ringe, D., & Petsko, G. A. (1988) *Proceedings of the American Society for Microbiology Meeting on Genetics and Molecular Biology of Industrial Microorganisms*, Bloomington, IN, Oct 2–7, 1988, American Society for Microbiology, Washington, DC (in press).

Tucker, M. Y., Tucker, M. P., Himmel, M. E., Grohmann, K., & Lastick, S. M. (1988) *Biotechnol. Lett. 10*, 79.

Vangrysperre, W., Callens, M., Kersters-Hilderson, H., & DeBruyne, C. K. (1988) *Biochem. J. 250*, 153.

Volk, W. A. (1966) *Methods Enzymol. 9*, 585.

Warnhoff, E. W., Reynolds-Warnhoff, P., & Wong, M. Y. H. (1980) *J. Am. Chem. Soc. 102*, 5957.

Wilhelm, M., & Hollenberg, C. P. (1984) *EMBO J. 3*, 2555.

Wilhelm, M., & Hollenberg, C. P. (1985) *Nucleic Acids Res. 13*, 5717.

Yamanaka, K. (1969) *Arch. Biochem. Biophys. 131*, 502.

Yamanaka, K., & Izumori, K. (1975) *Methods Enzymol. 92*, 462.